PHYSICAL REVIEW B

CONDENSED MATTER

THIRD SERIES, VOLUME 49, NUMBER 14 1 APRIL 1994-II

Evaluation of time-differential measurements of nuclear-resonance scattering of x rays

W. Sturhahn* and E. Gerdau

II. Institute for Experimental Physics, University of Hamburg, D-22761 Hamburg, Germany

(Received 19 July 1993; revised manuscript received 8 December 1993)

Time-differential measurements of nuclear-resonance scattering using synchrotron radiation sources have been performed since 1984. In the present contribution the evaluation of this type of spectra is described. Starting from the theoretical point of view numerical methods are applied to gain hyperfine interaction parameters from time spectra. The CONUSS program package that was developed can be used to interpret either nuclear Bragg-Laue scattering or nuclear forward scattering. It is also possible to investigate combinations of several resonant samples which is important for comparing measurements.

INTRODUCTION

The large storage rings of high-energy physics are the brightest x-ray sources available. The emitted synchrotron radiation (SR) has an energy bandwidth of about 30 keV at the existing rings and it will be shifted within the next years up to 100 keV or even more. Therefore, low-lying nuclear resonances—the Mössbauer (MB) levels—can be excited. The proposal to use SR to observe recoilless resonant scattering (MB effect) by Ruby[1] marks the starting point of the evolution of MB spectroscopy with SR. Up to now, several experiments have been performed that demonstrated how to use high brilliance, time structure, and polarization of SR for resonant scattering.[2–6] It was especially useful to observe the decay of the nuclear exciton in the time domain. In fact, the time evolution of nuclear resonance scattering after SR pulse excitation is scaled by the lifetime of the nuclear resonance (e.g., ^{57}Fe, 143 ns; ^{119}Sn, 25.7 ns, ^{169}Tm, 5.8 ns). The time resolution of existing x-ray detectors ($\lesssim 1.5$ ns) provides the possibility to filter the photons scattered by nuclei simply by observing the delayed photons only. This improves the signal-to-noise ratio considerably and appears to be the key technique for nuclear-resonance scattering experiments with SR.

Ultrahigh-brilliance SR sources like ESRF, APS, or Spring8 will enable us to gain appreciable progress in spectroscopic application of the method. The evolution will strongly be influenced by the existence and availability of evaluation programs. Indeed, an accurate measurement must be analyzed in a proper way to gain new and important results. To face this demand, the CONUSS (coherent nuclear scattering from single crystals) program package was developed.

The observed time spectra can be regarded as coherent elastic scattering of SR in a narrow energy range which is defined by the width of the excited nuclear level and some additional broadening due to multiple scattering. Theories that elaborate coherent elastic scattering in case of sharp nuclear resonances have been developed by Hannon and Trammell[17,18] and Afanasev and Kagan.[19,20] Also a brief outline has been given by one of the authors.[21] These theories are complicated enough to make a numerical analysis necessary.

In the present paper, we will follow the approach of Hannon and Trammell in general and Ref. 21 in detail. First, the elastic scattering amplitudes of a single atom in a solid are calculated. This will already contain all dependences of the nuclear-resonance scattering on the hyperfine interaction. The next step will be to combine the scattering amplitudes of several atoms coherently. We will assume very thin platelets to avoid the mathematical problems arising from multiple scattering effects. This is equivalent to the first Born approximation (kinematical approximation). The combination of a large number of such platelets includes the effects of multiple scattering and will lead us to Bragg-Laue scattering or, in a more simple case, to forward scattering. The coherent elastic scattering of a platelet is described by a 2×2 matrix, which arises from the two independent transverse polarizations of the incident photon. Additionally, each matrix element is dependent on the energy and direction of the incident photon.

This formulation allows the specification of the source properties explicitly. Thus, the scattering response due to illumination of resonant materials by synchrotron radiation is easily derived once the four matrix elements and their dependencies mentioned above have been calculated. Either energy or time representation of the resulting scattering amplitudes are equivalent. CONUSS offers both possibilities in addition to being able to calculate conventional transmission spectra. In fact, the transmission in-

tegral introduced by Margulies and Ehrmann[22] and also by Harris[23] entirely involves multiple scattering effects in the special case of forward scattering. As the intention of CONUSS is more general we refer to the program package WOTAN, which is a highly developed fitting procedure for conventional transmission spectra.[24]

The problem of linking a rather complex theoretical approach to the needs of evaluating time-differential measurements by experimentalists is treated in the present contribution. The underlying principles and the numerical approach as realized in the CONUSS program package are discussed. The source code is written in FORTRAN77. The program was tested for about 5 years by evaluating time differential measurements performed at HASYLAB. The CONUSS program package is freely available from the authors.[25]

ELASTIC SCATTERING BY A MÖSSBAUER ATOM

Here, the interaction between a photon field and the electromagnetic currents of a solid scatterer will be discussed. The photon field has to be quantized as demanded by the theory of quantum electrodynamics. But due to the low density of photon modes of common x-ray sources, it is sufficient to investigate the behavior of photon fields with only one mode occupied by a single photon. In this case, the photon field is described classically as linear superposition of plane waves. Because the distribution of electromagnetic currents in a solid may be very complicated, it is worthwhile to discuss first the scattering behavior of a single atom. The scattered field of an atom in phase space is given by

$$[\tilde{A}_\mu^{(S)}(\mathbf{k},\omega)]_{fi}=-c\frac{\tilde{\delta}_+(k,\omega)}{(2\pi)^4}\int\langle\Psi_f|\tilde{\mathbf{M}}_{\mu\nu}(\mathbf{k},\omega;\mathbf{k}',\omega')|\Psi_i\rangle\,\tilde{A}_0^\nu(\mathbf{k}',\omega')d^3k'd\omega'\ ,$$

$$\tilde{\mathbf{M}}_{\mu\nu}(\mathbf{k},\omega;\mathbf{k}',\omega')=\frac{i}{c}\int e^{-i(\mathbf{kx}-\omega t)}e^{i\mathbf{H}t}\mathbf{b}_\mu(\mathbf{x})\mathbf{G}(t-t')\mathbf{b}_\nu(\mathbf{x}')e^{-i\mathbf{H}t'}e^{i(\mathbf{k}'\mathbf{x}'-\omega't')}d^3xd^3x'dtdt'\ , \tag{1}$$

$$\tilde{\delta}_+(k,\omega)=-\frac{4\pi c}{\omega^2-k^2c^2+i\epsilon}\ .$$

Here and in the following equations, we use Greek indices to describe transverse components of the photon fields, and we apply the sum rule of Einstein. The incoming field is represented by $\tilde{A}_0^\nu(\mathbf{k},\omega)$, which may be understood as the wave function of a photon. In fact, $|\tilde{A}_0^\nu(\mathbf{k},\omega)|^2d^3kd\omega$ is the probability of finding the incoming photon in the mode characterized by the wave vector $\mathbf{k}$, energy $\hbar\omega$, and polarization ν. $\tilde{\delta}_+$ is the propagator of an outgoing photon. $|\Psi_{i,f}\rangle$ is the eigenstate of the solid before and after the scattering process. $\tilde{\mathbf{M}}_{\mu\nu}$ is called the scattering operator of the atom. It depends on the electromagnetic currents $\mathbf{b}_\mu$, on the Hamiltonian $\mathbf{H}$, and on the propagator $\mathbf{G}$ of the atom. The propagator itself can be expressed in terms of the Hamiltonian and an operator $\tilde{\mathbf{\Delta}}$, which describes the (small) perturbation of the atom by the photon field:

$$\mathbf{G}(t-t')=\frac{i}{2\pi}\int\frac{e^{-i\omega(t-t')}}{\omega-\mathbf{H}-\tilde{\mathbf{\Delta}}(\omega)}d\omega\ . \tag{2}$$

The real part of the perturbation operator leads to a shift of the atomic energy levels which is negligible in this context. The imaginary part gives the lifetime $\bar{t}$ of an intermediate atomic state $|\Psi_n\rangle$:

$$(\bar{t})^{-1}=-2\,\mathrm{Im}\{\langle\Psi_n|\tilde{\mathbf{\Delta}}|\Psi_n\rangle\}\ . \tag{3}$$

The smaller this imaginary contribution becomes, the more pronounced is the resonance behavior of the propagator for a given intermediate state. This leads to a strong enhancement of the scattering in the vicinity of sharp nuclear resonances.

In the following, we will restrict ourselves to the calculation of the diagonal elements of the operator $\tilde{\mathbf{M}}_{\mu\nu}$, which describe elastic scattering. The currents $\mathbf{b}_\mu$ of the atom are split into the nuclear and the electronic part. This gives three contributions to the scattering operator: the pure electronic part, the pure nuclear part, and an interference term between the nuclear and electronic currents. For calculation of the first term, we assume scattering to take place far off any resonances of the electron shell. This kind of electronic scattering is slowly varying in energy and conserves the polarization of the incoming photon. With the atom located at $\mathbf{R}$ the well-known result is

$$\tilde{E}_{\mu\nu}(\mathbf{k},\omega;\mathbf{k}',\omega')=2\pi\delta_{\mu\nu}\delta(\omega'-\omega)F_{\mathrm{DW}}e^{i(\mathbf{k}'-\mathbf{k})\mathbf{R}}\times\left[-r_0F_e(\mathbf{k}'-\mathbf{k})+i\frac{k}{4\pi}\sigma_{\mathrm{pe}}(\omega)\right]\ . \tag{4}$$

The Debye-Waller factor F_{DW} describes the reduction of probability for elastic scattering due to interaction of the atom with the lattice in which it is bound. Introducing this factor we made use of the adiabatic approximation, that is the eigenstate of the electron shell is assumed to adjust immediately to the nuclear motion. r_0 is the classical electron radius, F_e the form factor of the electron shell, and σ_{pe} the photoelectric cross section of the atom. The values of F_e and σ_{pe} are tabulated.[26,27] These tables have been included in the CONUSS program.

The description of nuclear-resonance scattering is more complicated. We assume the lifetime of the nuclear resonance to be large in comparison to typical lattice vibration periods. Then the nuclear contribution is scaled by the well-known Mössbauer-Lamb factor and we get

$$\tilde{N}_{\mu\nu}(\mathbf{k},\omega;\mathbf{k}',\omega')=\frac{1}{c}F_{\mathrm{ML}}\delta(\omega'-\omega)e^{i(\mathbf{k}'-\mathbf{k})\mathbf{R}}\sum_n \frac{\langle\phi_i|\mathbf{J}_\mu(-\mathbf{k})|\phi_n\rangle\langle\phi_n|\mathbf{J}_\nu(\mathbf{k}')|\phi_i\rangle}{\Omega_n-\Omega_i-\omega'-i\Lambda_{ni}} \ . \tag{5}$$

Here the Fourier components $\mathbf{J}_\mu$ of the nuclear currents in the center-of-mass system (CMS) of the atom have been introduced. In the CMS, the eigenstates and eigenenergies of the atom have been labeled $|\phi\rangle$ and $\hbar\Omega$. The sum includes all possible intermediate states of the atom. The resonance width Λ_{ni} is given as a matrix element of the perturbation operator $\tilde{\Delta}$:

$$\Lambda_{ni}=-\mathrm{Im}\{\langle\phi_n|\tilde{\Delta}(\Omega_i+\omega')|\phi_n\rangle\} \ . \tag{6}$$

In the vicinity of a sharp nuclear resonance (which means $\Omega_i+\omega'\approx\Omega_n$), the matrix element Λ_{ni} is given by the natural linewidth $\Gamma_0=2\hbar\Lambda_{ni}$.

Usually the excitation of a nucleus is described in terms of multipole radiation. Therefore, a multipole expansion of the nuclear currents is extremely useful. For calculation of the arising matrix elements, it is necessary to make assumptions about the interaction between the nucleus, the electron shell, and the rest of the solid. We will restrict ourselves to the cases that are known as fast relaxation limit and slow relaxation limit. Then, the interaction between the nucleus and electrons may be taken as independent of time. The energies $\hbar\Omega$ and the wave functions $|\phi\rangle$ occurring in Eq. (5) now describe a nucleus under the influence of static hyperfine fields. In this case, it is convenient to use a set of eigenstates $\{|\mathrm{Im}\rangle\}$ of the nuclear spin operator for the representation of the nuclear wave functions. This leads to

$$\tilde{N}_{\mu\nu}(\mathbf{k},\omega;\mathbf{k}',\omega')=\frac{\pi(2I_n+1)}{k}F_{\mathrm{ML}}\delta(\omega'-\omega)e^{i(\mathbf{k}'-\mathbf{k})\mathbf{R}}\sum_{LL'\lambda\lambda'}\delta_{L\lambda}\delta^*_{L'\lambda'}\sum_n \frac{[\mathbf{T}^{(\lambda)}_{Lni}(\hat{k})]^*_\mu[\mathbf{T}^{(\lambda')}_{L'ni}(\hat{k}')]_\nu}{z_{ni}(\omega')-i} \ , \tag{7}$$

with

$$\mathbf{T}^{(\lambda)}_{Lni}(\hat{k})=\left[\frac{8\pi}{2I_n+1}\right]^{1/2}\sum_{Mm}\mathbf{Y}^{(\lambda)*}_{LM}(\hat{k})C(I_iLI_n;mN)\langle I_im|\phi_i\rangle\langle\phi_n|I_nm+M\rangle \ ,$$

$$z_{ni}(\omega')=\frac{2\hbar}{\Gamma_0}(\Omega_n-\Omega_i-\omega') \ .$$

$I_{i,n}$ are the nuclear spins of the ground state and excited state. $\mathbf{Y}^{(\lambda)}_{LM}$ represents the vector spherical harmonics, $C(\cdots)$ the Clebsch-Gordan coefficients in the notation of Rose.[28] $\delta_{L\lambda}$ are the multipole mixing coefficients. They are normalized to the total internal conversion coefficient α of the transition:

$$(1+\alpha)\sum_{L\lambda}|\delta_{L\lambda}|^2=1 \ . \tag{8}$$

Usually one multipolarity predominates. Then for an $(L\lambda)$ multipole transition, the matrix elements of the nuclear scattering operator are given by

$$\tilde{N}_{\mu\nu}(\mathbf{k},\omega;\mathbf{k}',\omega')=\frac{\pi(2I_n+1)}{k(1+\alpha)}F_{\mathrm{ML}}\delta(\omega'-\omega)e^{i(\mathbf{k}'-\mathbf{k})\mathbf{R}}\sum_n \frac{[\mathbf{T}^{(\lambda)}_{Lni}(\hat{k})]^*_\mu[\mathbf{T}^{(\lambda)}_{Lni}(\hat{k}')]_\nu}{z_{ni}(\omega')-i} \ . \tag{9}$$

For the Mössbauer isotopes of ^{57}Fe, ^{169}Tm, and ^{119}Sn, nearly pure $M1$ Mössbauer transitions are observed. This corresponds to $L=1$ and $\lambda=0$.

The nuclear contribution to the x-ray scattering of an atom depends strongly on energy. The energy range in which strong scattering occurs is determined by the natural linewidth Γ_0 and by the nuclear level splitting given by $\hbar(\Omega_n-\Omega_i)$.

The interference terms between nuclear and electronic currents gives a small correction of the nuclear contribution in Eq. (7). They are included in a satisfactory way by a substitution of the multipole mixing coefficients as calculated by Goldwire and Hannon:[29]

$$\delta_{L\lambda}\delta^*_{L'\lambda'}\rightarrow\delta_{L\lambda}\delta^*_{L'\lambda'}(1+E_{L\lambda})(1+E_{L'\lambda'})$$

with

$$|E_{L\lambda}|\ll 1 \ , \tag{10}$$

whereas the real part of $E_{L\lambda}$ is fairly negligible, the imaginary part changes the shape of the resonant response. Introducing $\beta_{L\lambda}=2\,\mathrm{Im}\{E_{L\lambda}\}$, the nuclear scattering matrix including interference terms reads

$$\tilde{N}_{\mu\nu}(\mathbf{k},\omega;\mathbf{k}',\omega')=\frac{\pi(2I_n+1)}{k(1+\alpha)}F_{\mathrm{ML}}\delta(\omega'-\omega)e^{i(\mathbf{k}'-\mathbf{k})\mathbf{R}}(1+i\beta_{L\lambda})\sum_n \frac{[\mathbf{T}^{(\lambda)}_{Lni}(\hat{k})]^*_\mu[\mathbf{T}^{(\lambda)}_{Lni}(\hat{k}')]_\nu}{z_{ni}(\omega')-i} \ . \tag{11}$$

This equation and the electronic part given in Eq. (4) sum up to the elastic scattering matrix of the whole atom.

The elastic scattering from a Mössbauer atom depends on the direction and polarization of the incoming and outgoing photon, the energy of the photon, and the interaction between the nucleus and electrons. The effect of the interaction between the nucleus and electrons is to influence the hyperfine interaction and therefore the nuclear eigenstates and eigenenergies. Because of the sharp resonance of the nuclear contribution, the elastic scattering is very sensitive to the hyperfine interaction. In addition, strong polarization mixing occurs, which is described by the scattering strengths $[\mathbf{T}^{(\lambda)}_{Lni}(\hat{k})]_\mu$ of the possible excitations of the nucleus according to the properties of the scattered photon. How nuclear eigenenergies, nuclear eigenstates, and the vector spherical harmonics that have to be combined to give the scattering strengths are calculated by CONUSS will be discussed in more detail.

Using the same set of eigenstates $\{|nI_n m\rangle\}$ of the nuclear spin operator as in Eq. (7), we get the following matrix elements of the different multipole orders of the hyperfine interaction Hamiltonian:

$$\begin{aligned}
&\hbar\langle \mathrm{Im}|\mathbf{H}^{(0)}_{\mathrm{hf}}|\mathrm{Im}'\rangle = \delta_{mm'}E_0 \ , \\
&\hbar\langle \mathrm{Im}|\mathbf{H}^{(1)}_{\mathrm{hf}}|\mathrm{Im}'\rangle = -\mu B_{\mathrm{hf}}(-1)^{m-m'}\frac{C(I1I;m,m'-m)}{C(I1I;I0)}\mathcal{D}^{(1)}_{0,m-m'}(0,\theta,\varphi) \ , \\
&\hbar\langle \mathrm{Im}|\mathbf{H}^{(2)}_{\mathrm{hf}}|\mathrm{Im}'\rangle = \frac{eqV_{zz}}{2}(-1)^{m-m'}\frac{C(I2I;m,m'-m)}{2C(I2I;I0)}\left[\mathcal{D}^{(2)}_{0,m-m'}(\alpha,\beta,\gamma)\right. \\
&\qquad\qquad \left. +\frac{\eta}{\sqrt{6}}[\mathcal{D}^{(2)}_{2,m-m'}(\alpha,\beta,\gamma)+\mathcal{D}^{(2)}_{-2,m-m'}(\alpha,\beta,\gamma)]\right] .
\end{aligned} \tag{12}$$

E_0 gives the isomer shift. μ is the magnetic dipole moment of the nucleus, and B_{hf} the magnetic hyperfine field. The angles θ and ϕ are the spherical coordinates of the direction of the magnetic hyperfine field in the (arbitrarily) chosen quantization system. q is the electric quadrupole moment of the nucleus. V_{zz} is the largest eigenvalue of the electric-field gradient tensor, and η is the asymmetry parameter of the EFG. α, β, γ denote the Euler angles that give the rotation from the system of the EFG main axes to the quantization system. All rotations are performed by the rotation matrices $\mathcal{D}^{(L)}_{mm'}$ as defined by Rose.[28]

This representation of the Hamiltonian of hyperfine interaction is convenient but generally not diagonal. This implies that the actual nuclear states are no longer eigenstates of the spin projection operator.[30]

In order to get a representation that can be handled numerically a quantization system has to be chosen. In the CONUSS routines we use the main axes system of the EFG because of the simplification of the Hamiltonian matrix elements in Eq. (12). For the sum of the multipole orders of these elements we get

$$\begin{aligned}
\hbar H_{mm'} = {} & \delta_{mm'}E_0 + (-1)^{m-m'+1}\mu B_{\mathrm{hf}}\frac{C(I1I;m,m'-m)}{C(I1I;I0)}\mathcal{D}^{(1)}_{0,m-m'}(0,\theta,\varphi) \\
& +(-1)^{m-m'}\frac{eqV_{zz}}{2}\frac{C(I2I;m,m'-m)}{2C(I2I;I0)}\left[\delta_{mm'}+\frac{\eta}{\sqrt{6}}\delta_{mm'\pm 2}\right] .
\end{aligned} \tag{13}$$

The coefficients of the nuclear eigenstates $u_{mj} = \langle \mathrm{Im}|\phi_j\rangle$ and the energy shifts E_j of the nuclear levels are solutions of the following eigenvalue problem:

$$\begin{aligned}
E_j\delta_{jj'} &= \sum_{mm'} u_{jm}(\hbar H_{mm'} - \delta_{mm'}E_0)u_{m'j'} \ , \\
\delta_{jj'} &= \sum_{mm'} u_{jm}u_{m'j'} \ .
\end{aligned} \tag{14}$$

For an arbitrary spin of the nuclear state, this system of equations cannot be solved analytically. Therefore, CONUSS uses an iterative diagonalization algorithm proposed by Eberlein.[31]

The calculation of the vector spherical harmonics in this quantization system is straightforward. For the sake of convenience, a linear base of polarization is used. If we denote the two orthonormal vectors by $\hat{\epsilon}_\mu$, $\mu = 1,2$, the components of the vector spherical harmonics are given by

$$\hat{\epsilon}_\mu \mathbf{Y}^{(\lambda)}_{LM} = (i)^{\mu+1}\left[\frac{2L+1}{16\pi}\right]^{1/2}\{\mathcal{D}^{(L)}_{1M} - (-1)^{\lambda+\mu}\mathcal{D}^{(L)}_{-1M}\} . \tag{15}$$

The argument of the rotation matrices are the Euler angles which rotate the photon system given by $\hat{k},\hat{\epsilon}_1,\hat{\epsilon}_2$ to the quantization system. Thus, with a proper set of parameters describing the atom the elastic scattering amplitude of Eq. (9) is calculated as a function of the properties of the incoming and outgoing photon.

COHERENT SCATTERING FROM THIN PLATELETS

The scattering of x rays by a solid may take place coherently or incoherently. From the microscopic point of view, this is due to whether the quantum state of the part of the solid that acts as scatterer is changed. This part may be a region in space, the whole solid, or only one atom. If we consider lattice vibrations the spatial region that acts coherently is given by the spatial coherence of the phonon that is created or annihilated in the scattering process. The usual case is a thermally excited solid. Then the spatial coherence length of phonons is of the order of the interatomic distance. An equivalent interpretation of this behavior is that vibrations of neighboring atoms are not correlated. In this scenario, inelastic coherent scattering is ruled out. The only remaining

coherent scattering process occurs elastically without phonon creation or annihilation. The influence of temperature will be taken into account by averaging over the initial atomic states with an appropriate Boltzmann factor. The reduction of the scattering amplitude due to inelastic scattering is given by the Mössbauer-Lamb factor and the Debye-Waller factor.

The assumption that scattering of a single photon mode by a solid is described by the sum of the contributions of the individual atoms is fairly justified in the x-ray case by calculations of Hannon and Trammell.[17] They also proved that mirror terms that arise from virtual photon exchange between two atoms lead to a minor contribution and can be neglected. We will take the thermal average over all initial nuclear states at a temperature very much larger than their splitting. For an incident monochromatic plane wave field with wave vector $\mathbf{k}_0$, energy $\hbar\omega_0=\hbar ck_0$, and amplitude $a_{0,\nu}$, we get for the scattering amplitude of a thin platelet:

$$\tilde{A}_\mu^{(S)}(\mathbf{k},\omega)=-c\tilde{\delta}_+(k,\omega)\sum_j e^{i(\mathbf{k}_0-\mathbf{k})\mathbf{R}_j}\tilde{M}_{\mu\nu}^{\prime(j)}(\mathbf{k},\omega;\mathbf{k}_0,\omega)\delta(\omega-ck_0)\bar{a}_{0,\nu}\ ,$$

with

$$\tilde{M}_{\mu\nu}^{\prime(j)}(\mathbf{k},\omega;\mathbf{k}_0,\omega)=\frac{k_0}{2}\sigma_0 F_{\mathrm{ML}}^{(j)}(1+i\beta_{L\lambda})\sum_{ni}^{(j)}\frac{[\mathbf{T}_{Lni}^{(\lambda)}(\hat{k})]_\mu^*[\mathbf{T}_{Lni}^{(\lambda)}(\hat{k}_0)]_\nu}{z_{ni}(\omega)-i}+2\pi F_{\mathrm{DW}}^{(j)}\delta_{\mu\nu}\left[-r_0F_e^{(j)}(\mathbf{k}_0-\mathbf{k})+i\frac{k}{4\pi}\sigma_{pe}^{(j)}(\omega)\right]\ . \quad (16)$$

The sum over j has to be taken over all atoms of the platelet. σ_0 is the nuclear-resonance cross section. Equation (16) clearly neglects multiple scattering but is a very good approximation because the intensity of the scattered radiation is small in comparison to the incident radiation. It is the first Born or kinematical approximation. Next, we consider thin platelets for which this approximation is sufficient.

A look at Eq. (16) reveals that for $|\mathbf{k}-\mathbf{k}_0|\neq 0$, the spatial positions of the atoms in the platelet are of importance. On the other hand, in the case of forward scattering ($|\mathbf{k}-\mathbf{k}_0|=0$), it does not matter whether the material is ordered or not. Thus, CONUSS performs calculations for the more general case of an ordered material. Forward scattering even for polycrystalline or amorphous materials is automatically included. The sum over all atoms that occurs in Eq. (16) can be split into a sum over the unit cell of the ordered material and a sum over all unit cells in the platelet. We get

$$\sum_j e^{i(\mathbf{k}_0-\mathbf{k})\mathbf{R}_j}\tilde{M}_{\mu\nu}^{\prime(j)}=\tilde{M}_{\mu\nu}^{(uc)}\sum_j e^{i(\mathbf{k}_0-\mathbf{k})\mathbf{v}_j}\ . \quad (17)$$

The positions of the unit cells are given by $\mathbf{v}_j$, and $\tilde{M}_{\mu\nu}^{(uc)}$ denotes the scattering matrix of the unit cell. It is given by the position and kind of the atoms in the unit cell. If $\mathbf{r}_j$ is a possible position in the unit cell and p_{aj} is the probability to find this position occupied by an atom of kind a, we may write

$$\tilde{M}_{\mu\nu}^{(uc)}=\sum_{aj}p_{aj}e^{i(\mathbf{k}_0-\mathbf{k})\mathbf{r}_j}\tilde{M}_{\mu\nu}^{\prime(a)}\ . \quad (18)$$

The sum over all unit cells can be written as a sum of δ functions if we assume that the dimensions of the platelet perpendicular to the surface normal are large compared with the range of x rays in the material. Introducing the planar reciprocal lattice vectors of the platelet $\mathbf{g}_\tau$, we get

$$\sum_j e^{i(\mathbf{k}_0-\mathbf{k})\mathbf{R}_j}\tilde{M}_{\mu\nu}^{\prime(j)}=\tilde{M}_{\mu\nu}^{(uc)}\frac{(2\pi)^2 b}{V_{\mathrm{uc}}}\sum_\tau\delta^2(\mathbf{k}_{0xy}-\mathbf{k}_{xy}-\mathbf{g}_\tau)\ . \quad (19)$$

In this equation the indices xy denote the component perpendicular to the surface normal of the platelet. V_{uc} is the volume of a unit cell, and b is the thickness of the platelet. The scattered field is then given as a sum over the contributions from each reciprocal-lattice vector. After inserting this result into Eq. (16) we perform a Fourier transformation to obtain the scattered photon field in space and time. We get wave fields only for those reciprocal-lattice vectors $\mathbf{g}_\tau$ that fulfill the condition $|\mathbf{k}_{0xy}+\mathbf{g}_\tau|\leq k_0$. Finally we get

$$A_\mu^\pm(\mathbf{x},t)=ib\sum_\tau e^{i(\mathbf{k}_{\tau\pm}\mathbf{x}-\omega_0 t)}f_{\mu\nu}^{\tau\pm 0^+}a_{0,\nu}$$

with

$$\mathbf{k}_{\tau\pm}=\mathbf{k}_{0xy}+\mathbf{g}_\tau\pm\hat{z}\sqrt{k_0^2-(\mathbf{k}_{0xy}+\mathbf{g}_\tau)^2}\ ,$$
$$f_{\mu\nu}^{\tau\pm 0^+}=\frac{\tilde{M}_{\mu\nu}^{(uc)}(\mathbf{k}_\tau^\pm,\omega_0;\mathbf{k}_0,\omega_0)}{V_{\mathrm{uc}}(\mathbf{k}_{\tau\pm})_z}\ . \quad (20)$$

The plus sign hold for $\hat{z}\mathbf{x}\geq 0$ if the surface normal of the platelet is denoted by $\hat{z}$ with $\hat{z}\mathbf{k}_0>0$. Thus, the scattered wave field is a superposition of plane waves with frequency $\omega_0=ck_0$ and with wave vectors $\mathbf{k}_{\tau+}$ or $\mathbf{k}_{\tau-}$ below or above the platelet. In this notation, $\mathbf{k}_{0^+}$ and $\mathbf{k}_0$ are identical. Furthermore, we introduced the planar scattering amplitudes $f_{\mu\nu}^{\tau\pm 0^+}$, which express the coupling of a ν polarized photon propagating in the 0^+ channel to a μ polarized photon propagating in the $\tau^\pm$ channel. Note that the polarization indices refer to the same reference system thus leading to an additional projection factor if different polarization bases are chosen for incident and scattered photons.

ELASTIC SCATTERING FROM REAL SAMPLES

Samples that are investigated experimentally do not obey the rules for "thin" scatterers. This implies that the first Born approximation is no longer valid for the scattered fields, and multiple scattering has to be considered.

Bragg scattering of thick crystals or transmission through absorbers of appreciable thickness may serve as examples. Up to this point, we calculated scattering amplitudes for thin platelets, which we could derive from the density, position, and properties of the atoms. It is straightforward to use these results for the calculation of the scattering amplitudes of a thick platelet. We apply the trick of cutting up the crystal into thin platelets that are equivalent. The displacement of the platelets in the direction of the surface normal $\hat{z}$ is then mb, where m is the platelet number that counts from $m=0$ (upper surface of the crystal) to $m=D/b$ (D is the thickness of the crystal). The change of the fields of the $\tau^{\pm}$ channels from one platelet to the next is then given by

$$A_{\mu}^{\tau^+}(m+1)=e^{ib\sqrt{k_0^2-(\mathbf{k}_{0xy}+\mathbf{g}_{\tau})^2}}\left[A_{\mu}^{\tau^+}(m)+ib\sum_{\tau'^{\pm}}f_{\mu\nu}^{\tau^+\tau'^{\pm}}A_{\nu}^{\tau'^{\pm}}(m)\right],$$

$$A_{\mu}^{\tau^-}(m-1)=e^{ib\sqrt{k_0^2-(\mathbf{k}_{0xy}+\mathbf{g}_{\tau})^2}}\left[A_{\mu}^{\tau^-}(m)-ib\sum_{\tau'^{\pm}}f_{\mu\nu}^{\tau^-\tau'^{\pm}}A_{\nu}^{\tau'^{\pm}}(m)\right]$$

with

$$f_{\mu\nu}^{\tau^{\pm}\tau'^{\pm}}=\frac{\tilde{M}_{\mu\nu}^{(uc)}(\mathbf{k}_{\tau^{\pm}},\omega_0;\mathbf{k}_{\tau'^{\pm}},\omega_0)}{V_{uc}(\mathbf{k}_{\tau^{\pm}})_z}\ . \tag{21}$$

These equations determine the photon fields inside the crystal recursively. The deviations of the wave vectors from the result of the first Born approximation are expected to be small. Thus, a phase factor may be split off leaving a field amplitude that varies only slowly in space:

$$A_{\mu}^{\tau^{\pm}}(m)=e^{i[(\mathbf{k}_0+\mathbf{G}_{\tau})\mathbf{x}_m-\omega_0 t]}a_{\mu}^{\tau^{\pm}}(m)\ . \tag{22}$$

$\mathbf{G}_{\tau}$ is a reciprocal-lattice vector of the crystal. This substitution leaves Eq. (21) in the following form:

$$a_{\mu}^{\tau^+}(m+1)=e^{ib\kappa_{\tau^+}}\left[a_{\mu}^{\tau^+}(m)+ib\sum_{\tau'^{\pm}}f_{\mu\nu}^{\tau^+\tau'^{\pm}}a_{\nu}^{\tau'^{\pm}}(m)\right],$$

$$a_{\mu}^{\tau^-}(m-1)=e^{-ib\kappa_{\tau^-}}\left[a_{\mu}^{\tau^-}(m)-ib\sum_{\tau'^{\pm}}f_{\mu\nu}^{\tau^-\tau'^{\pm}}a_{\nu}^{\tau'^{\pm}}(m)\right],$$

with

$$\kappa_{\tau^{\pm}}=-(\mathbf{k}_0+\mathbf{G}_{\tau})_z\pm\sqrt{k_0^2-(\mathbf{k}_{0xy}+\mathbf{G}_{\tau xy})^2}\ . \tag{23}$$

The coupling of a field amplitude $a_{\mu}^{\tau^{\pm}}$ of a particular channel $\mathbf{k}_{\tau^{\pm}}$ to another channel $\mathbf{k}_{\tau'^{\pm}}$ becomes significant if the phase holds $|\sin b\kappa_{\tau^{\pm}}|\approx|bf^{\tau^{\pm}\tau'^{\pm}}|$. For a given direction of the incident wave vector, these channels are called open whereas the others are called closed. Note that the forward channel ($\mathbf{G}_0=0$) is always open because $\kappa_{0^+}=0$ for all directions of the incident radiation.

In experiments often only one or two open channels have to be considered. This is the case for simple forward scattering (only 0^+ channel open) or for Bragg scattering (0^+ and 1^- channel open) or for Laue scattering (0^+ and 1^+ channel open). CONUSS is able to deal with these three cases. Because our interest is restricted to the fields on top and at the bottom of the platelet, the following boundary conditions apply:

$$a_{\mu}^{\tau^+}(m=0)=a_{0,\mu}\delta_{0^+\tau^+}\ ,$$
$$a_{\mu}^{\tau^-}\left[m=\frac{D}{b}\right]=0\ . \tag{24}$$

The fields of the open channels are then solutions of the following set of differential equations:

$$da_{\mu}^{\tau^{\pm}}(z)=i\sum_{\tau'^{\pm}}(\kappa_{\tau^{\pm}}\delta_{\mu\nu}^{\tau^{\pm}\tau'^{\pm}}+f_{\mu\nu}^{\tau^{\pm}\tau'^{\pm}})a_{\nu}^{\tau'^{\pm}}(z)dz\ ,$$
$$a_{\mu}^{\tau^+}(0)=a_{0,\mu}\delta_{0^+\tau^+}\ , \tag{25}$$
$$a_{\mu}^{\tau^-}(D)=0\ .$$

The determination of the solutions is straightforward once the corresponding eigenvalue problem has been solved. CONUSS evaluates the eigenvalues k_n as roots of the following characteristic polynomial:

$$\det\{(\kappa_{\tau^{\pm}}-k_n)\delta_{\mu\nu}^{\tau^{\pm}\tau'^{\pm}}+f_{\mu\nu}^{\tau^{\pm}\tau'^{\pm}}\}=0\ . \tag{26}$$

The order of the polynomial is two times the number of open channels, which is four in the Bragg-Laue case and two for forward scattering. Vanishing polarization mixing in the Bragg-Laue case allows a factorization into two quadratic equations. This is handled separately to minimize computing time. In the general case, a numerical iteration of a damped Newton type is applied. A quality of better than 10^{-12} for each root is achieved. The eigenvectors $\alpha_{\mu n}^{\tau^{\pm}}$ are calculated from the following set of linear equations:

$$\sum_{\tau'^{\pm}}\{(\kappa_{\tau^{\pm}}-k_n)\delta_{\mu\nu}^{\tau^{\pm}\tau'^{\pm}}+f_{\mu\nu}^{\tau^{\pm}\tau'^{\pm}}\}\alpha_{\nu n}^{\tau^{\pm}}=0\ . \tag{27}$$

This system of linear equations is homogeneous, and thus the eigenvectors are determined up to an arbitrary factor. Therefore, one component of each eigenvector is set to unity. The leads to an inhomogeneous system of linear equations with reduced dimension, which is solved easily by the method of Gauss and Seidel. The field amplitudes at depth z_1 in the crystal $a_{\mu}^{\tau^{\pm}}(z_1)$ and the field amplitudes at the depth z_2 in the crystal $a_{\mu}^{\tau^{\pm}}(z_2)$ satisfy the following linear equations (no summations over μ):

$$\sum_{\tau^{\pm}}\alpha_{\mu n}^{\tau^{\pm}}a_{\mu}^{\tau^{\pm}}(z_2)=e^{ik_n(z_2-z_1)}\sum_{\tau^{\pm}}\alpha_{\mu n}^{\tau^{\pm}}a_{\mu}^{\tau^{\pm}}(z_1)\ . \tag{28}$$

If we take the boundary conditions of Eq. (25), the following equations determine the desired field amplitudes $a_{\mu}^{\tau^+}(D)$ and $a_{\mu}^{\tau^-}(0)$:

$$e^{-ik_n D}\sum_{\tau^+}\alpha_{\mu n}^{\tau^+}a_{\mu}^{\tau^+}(D)-\sum_{\tau^-}\alpha_{\mu n}^{\tau^-}a_{\mu}^{\tau^-}(0)=\alpha_{\mu n}^{0^+}a_{0,\mu}\ . \tag{29}$$

Note that a summation over the index μ need not be performed. In the CONUSS program, two orthogonal linear polarizations of the incoming radiation are assumed and the corresponding scattered field amplitudes are calculated. The choice of the polarization reference system depends on the scattering problem. In the case of forward scattering, the direction of an external field and the direction of the incoming γ quanta define a reference plane. σ polarization is then represented by the unit vector perpendicular to this plane. π polarization is then represented by the other transverse unit vector. This corresponds to the definition of Gonser and Fischer.[32] In the case of Bragg-Laue scattering, the reference plane is defined by incoming and scattered γ quanta. The definition of the polarization vectors is then the same as above. This is the usual definition from x-ray crystallography.

From Eq. (29), we obtain the field amplitudes as solutions for the two cases $a_{0,\sigma}=1$, $a_{0,\pi}=0$ and $a_{0,\sigma}=0$, $a_{0,\pi}=1$. The corresponding solutions are combined to 2×2 matrices that describe the field amplitudes of each open channel:

$$\tilde{T}^{\tau}=\begin{pmatrix} a_{\sigma}^{\tau^+}(\text{case 1}) & a_{\pi}^{\tau^+}(\text{case 1}) \\ a_{\sigma}^{\tau^+}(\text{case 2}) & a_{\pi}^{\tau^+}(\text{case 2}) \end{pmatrix}_{z=D},$$
$$\tilde{R}^{\tau}=\begin{pmatrix} a_{\sigma}^{\tau^-}(\text{case 1}) & a_{\pi}^{\tau^-}(\text{case 1}) \\ a_{\sigma}^{\tau^-}(\text{case 2}) & a_{\pi}^{\tau^-}(\text{case 2}) \end{pmatrix}_{z=0}. \tag{30}$$

This matrix description of the scattering behavior is especially useful if several samples are arranged in subsequent order. The total scattering matrix is then obtained by multiplication of those matrices that describe the used open channels. In this way, CONUSS allows the combination of Bragg-Laue reflections and forward scattering in arbitrary order.

SOURCE PROPERTIES AND SCATTERED INTENSITY

The total scattering matrix contains the entire dependence on energy and time. In the Bragg-Laue case, there is also a strong dependence on the angle of incidence θ of the incoming plane wave. On the other hand, for the evaluation of measured data in a given setup, the properties of the incoming radiation have to be defined. We will focus on synchrotron radiation sources. In the energy range of nuclear resonance scattering, the field amplitudes of incoming SR are independent of energy. This follows from the very short duration of typically 10^{-19} s of the emission process of photons in a synchrotron radiation beam. The time response of a scattering regime is then obtained by Fourier transformation of the total scattering matrix $\tilde{R}_{\text{total}}(\omega,\theta)$. The total scattering matrix is the product of matrices as given in Eq. (30) each describing one resonant scatterer of the regime. Our interest is restricted to observation of the nuclear-delayed part of the total scattering. Thus, it is reasonable to subtract the faroff resonance part $\tilde{R}_{\infty}(\theta)$, which is independent of energy, from the total scattering matrix. The time response of the regime due to nuclear scattering is then given by

$$R(t,\theta)=\int[\tilde{R}_{\text{total}}(\omega,\theta)-\tilde{R}_{\infty}(\theta)]e^{-i\omega t}d\omega\ . \tag{31}$$

Also, the degree and kind of polarization of the incoming radiation must be specified. We use the density matrix formalism and describe the polarization state of the incident beam by a 2×2 matrix ρ. The polarization analysis of the scattered photons is performed by a polarization filter which is described by the 2×2 matrix $\mathcal{P}$. We obtain for the time-dependent intensity

$$I(t,\theta)=\text{Tr}\{\rho R^{\dagger}\mathcal{P}^{\dagger}\mathcal{P}R\}\ . \tag{32}$$

For comparison with a measurement, three operations have to be added. First, the periodic bunching of SR has to be considered. This is done by adding the time-shifted intensities. The time shift t_S is given by the bunch distances in the synchrotron. This effect is of importance if the bunch separation is not much larger than the decay time of the scattering regime. Second, the divergence of the incident radiation and/or crystal bending is taken into account by a normalized distribution $W(\theta)$. Third, the time resolution of the detector system is given by a normalized distribution $T(t)$. The types of distributions that are implemented at present are rectangular, Lorentzian, symmetric Gaussian, and asymmetric Gaussian. For the intensity $\bar{I}$, which has to be compared to the measurement, we get

$$\bar{I}(t,\theta)=I_b+c\int\sum_{n\geq0}I(t'+nt_S,\theta')W(\theta-\theta')\times T(t+\Delta t-t')d\theta'dt'\ . \tag{33}$$

The background I_b, the scaling factor c, the angular position θ, the shift of the time scale Δt, and the widths of the distributions W and T are subject to a fitting procedure to minimize the χ^2 value as usual. χ^2 serves as measure for the quality of the fitted theory and its parameters.

APPLICATIONS

Measurements with high statistical accuracy that are performed with well-known samples are especially useful to verify theoretical calculations as described above. Until now, time-dependent nuclear resonance scattering was investigated in Bragg, Laue, and transmission geometry. The best quality of data was achieved by using pure nuclear reflections of single crystals.

The first example is a set of measurements of the pure nuclear reflection (002) of yttrium iron garnet ($Y_3Fe_5O_{12}$). The spectra are shown in Fig. 1 (data taken from Ref. 11). They were taken at different angles between the [100] crystal direction and the scattering plane while keeping the magnetization perpendicular to the scattering plane. This leads to variations of the hyperfine interactions due to changed angles between magnetic hyperfine field and main axis of the electric-field gradient. Therefore, we observe different quantum beat patterns. Details on the results of this evaluation are given in Ref. 33.

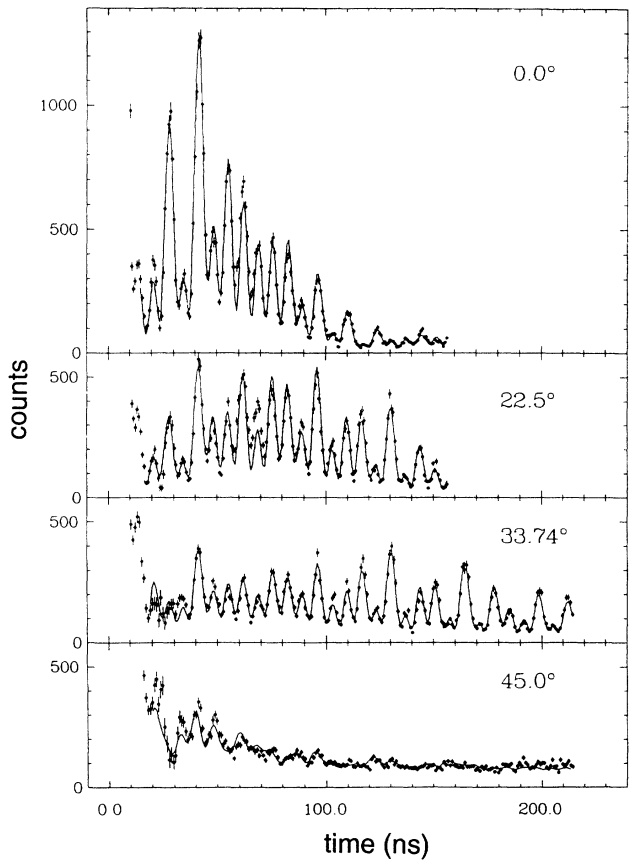

FIG. 1. The quantum beat pattern of the (002) pure nuclear reflection of YIG changes significantly with the angle between magnetic hyperfine field and main axes of the EFG. The calculations performed with CONUSS are shown as solid lines. The data are taken from Ref. 11.

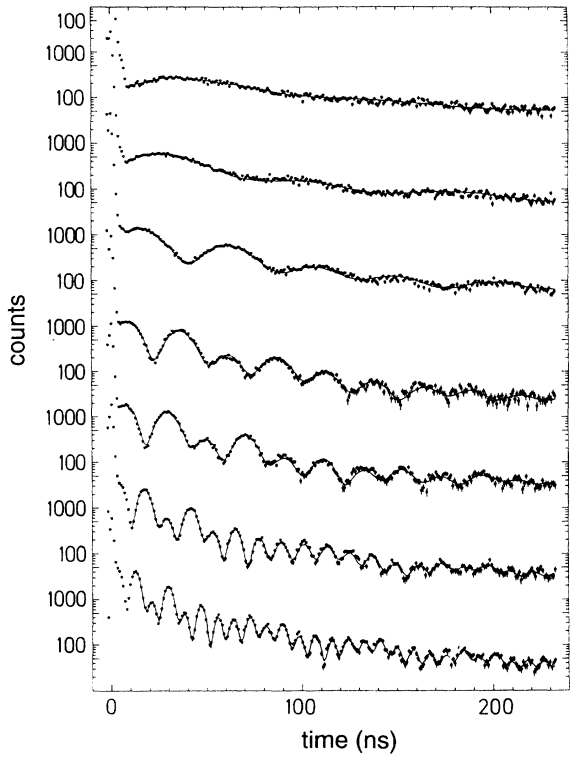

FIG. 2. The quantum beat pattern of the (333) pure nuclear reflection of iron borate is strongly influenced by the magnetic hyperfine field. This is shown for different temperatures in which the hyperfine field decreases approaching the Néel temperature. The calculations performed with CONUSS are shown as solid lines. The data are taken from Ref. 34.

The temperature dependence of the quantum beat pattern of the pure nuclear reflection (333) of iron borate ($FeBO_3$) is shown in Fig. 2 (data taken from Ref. 34). As the temperature approaches the Néel point, we observe an increasing quantum beat period that is directly correlated to the diminishing magnetic hyperfine fields. Details on the results of this evaluation are given in Ref. 33.

An experiment performed with a hematite crystal at the KEK undulator source demonstrates the use of nuclear diffraction at future synchrotron radiation sources.[35] The experimenters measured the quantum beat pattern of the (777) pure nuclear reflection with a resonant count rate of approximately 15 kHz and a very good suppression of the nonresonant prompt peak. The spectrum is shown in Fig. 3. The solid line represents the theoretical calculation obtained with CONUSS by defining two sublattices with partly different hyperfine interactions. The results of the fit procedure are given in Table I. The parameters for which errors are given were varied to give a minimum χ^2 of 56(8). In fact, this value is substantially larger than it should be if the errors of the measured data are of statistical nature. Systematic errors that superimpose the assumed statistical square-root errors are probably the reason. We assumed an asymmetric Gaussian shape for the response of the detector. The ratio of the widths before and after the maximum is 0.3 with a total of 2.22(4) ns FWHM. The angular divergence of the incoming beam was taken as symmetric Gaussian with a FWHM of 19.4(3) μrad. In fact, these shapes are probably not the best choice thus leading to

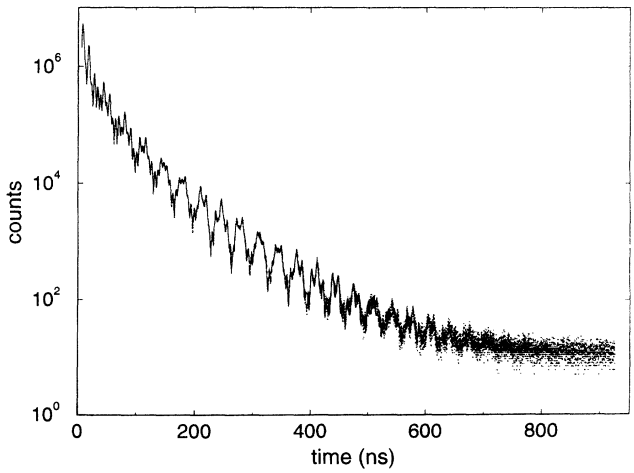

FIG. 3. The quantum beat pattern of the (777) pure nuclear reflection of hematite was measured very accurately. The calculation performed with CONUSS is shown as solid line. The data are taken from Ref. 37.

TABLE I. The hyperfine parameters of hematite as given by three different references. Blank positions indicate that no value was given for this parameter. Φ is the angle between the hyperfine fields of the two lattice sites. The f factor is the product of isotropic abundance and Mössbauer-Lamb factor.

Parameters	Ref.[a]	Ref.[b]	Ref.[c]
$\frac{1}{2}eqV_{zz}$ (mm s^{-1})	−0.40(2)	0.13(2)	−0.24(6)
B_{hf} (T)	51.56(3)	51.45(8)	51.5(5)
Φ (deg)	170.0(16)		
f factor	0.88(3)		
EFG axes	[111]		

[a]Present paper.
[b]Kikuta *et al.* (Ref. 35), same data but evaluated by Fourier transformation.
[c]Kistner *et al.* (Ref. 36), conventional MB transmission experiment with a polycrystalline sample.

systematic errors.

In future applications, it will be of considerable interest to evaluate time differential measurements taken in a forward scattering geometry. In advance to this situation, several cases of hyperfine interactions such as polycrystalline powders with and without external magnetic field are already implemented in CONUSS. Updates that will become available in the near future will include thickness averaging, relaxation effects due to nonstatic hyperfine interactions, and real fitting of the hyperfine parameters.

CONCLUSION

We extended the dynamical theory of MB optics of Hannon and Trammell[8] by allowing arbitrary static hyperfine interactions of the scattering nuclei. The special properties of nuclear-resonance scattering as energy dependence, polarization mixing, and angle dependence (in case of crystal reflections) are handled accurately on the basis of the given theory. Thus, phenomena like quantum beats, dynamical beats, and speed up that were addressed more empirically in several publications on time differential nuclear-resonance scattering are included in a general way in the equations given in the present contribution. The resulting description is formulated in a manner that allows conversion to computer source code easily. The numerical procedures (the CONUSS program package) were used to evaluate several time-differential measurements of nuclear Bragg scattering. It proved to be a powerful tool for understanding this kind of resonant scattering in the neV range. The excellent agreement between computed and measured data allows an accurate determination of hyperfine interaction parameters. The huge number of possibilities of setting up the calculation of nuclear resonance scattering addresses various kinds of experimental arrangements such as symmetric and asymmetric Bragg-Laue scattering, forward scattering, and any combination of different absorbers or crystal reflections. The flexible structure of the program package makes adaptations to different hardware and operating systems extremely easy to handle. The outstanding features of the CONUSS program package and its availability assign it an important role in a rather young but rising field of nuclear resonance scattering with SR.

ACKNOWLEDGMENTS

We would like to thank Dr. R. Hollatz for his worthwhile contributions while testing the CONUSS program package. We would like to acknowledge Professor J. P. Hannon for fruitful discussions. We also would like to thank Professor S. Kikuta and his working group for placing their data at our disposal. This work has been funded by the Bundesministerium für Forschung und Technologie under Contract No. 05 5GUAAI6, by the Deutsche Forschungsgemeinschaft under Contract No. Ge384/13-1, and in part by the U.S. Department of Energy BES-Materials Science under Contract No. W-31-109-ENG-38.

*Present address: Advanced Photon Source, Argonne National Laboratory, Argonne, Illinois 60439.

[1]S. L. Ruby, J. Phys. (Paris) Colloq. **35**, C6-209 (1974).
[2]E. Gerdau, R. Rüffer, H. Winkler, W. Tolksdorf, C. P. Klages, and J. P. Hannon, Phys. Rev. Lett. **54**, 835 (1985).
[3]E. Gerdau, R. Rüffer, R. Hollatz, and J. P. Hannon, Phys. Rev. Lett. **57**, 1141 (1986).
[4]U. van Bürck, R. L. Mössbauer, E. Gerdau, R. Rüffer, R. Hollatz, G. V. Smirnov, and J. P. Hannon, Phys. Rev. Lett. **59**, 355 (1987).
[5]R. Rüffer, E. Gerdau, R. Hollatz, and J. P. Hannon, Phys. Rev. Lett. **58**, 2359 (1987).
[6]G. Faigel, D. P. Siddons, J. B. Hastings, P. E. Haustein, J. R. Grover, J. P. Remeika, and A. S. Cooper, Phys. Rev. Lett. **58**, 2699 (1987).
[7]G. Faigel, D. P. Siddons, J. B. Hastings, P. E. Haustein, J. R. Grover, and L. E. Berman, Phys. Rev. Lett. **61**, 2794 (1988).
[8]D. P. Siddons, J. B. Hastings, G. Faigel, L. E. Berman, P. E. Haustein, and J. R. Grover, Phys. Rev. Lett. **62**, 1384 (1989).
[9]J. Arthur, G. S. Brown, D. E. Brown, and S. L. Ruby, Phys. Rev. Lett. **63**, 1629 (1989).
[10]J. B. Hastings, D. P. Siddons, G. Faigel, L. E. Berman, P. E. Haustein, and J. R. Grover, Phys. Rev. Lett. **63**, 2252 (1989).
[11]R. Rüffer, E. Gerdau, H. D. Rüter, W. Sturhahn, R. Hollatz, and A. Schneider, Phys. Rev. Lett. **63**, 2677 (1989).
[12]U. van Bürck, R. L. Mössbauer, E. Gerdau, W. Sturhahn, H. D. Rüter, R. Rüffer, A. I. Chumakov, M. V. Zelepukhin, and G. V. Smirnov, Europhys. Lett. **13**, 371 (1990).
[13]W. Sturhahn, E. Gerdau, R. Hollatz, R. Rüffer, H. D. Rüter, and W. Tolksdorf, Europhys. Lett. **14**, 821 (1991).
[14]J. B. Hastings, D. P. Siddons, U. v. Bürck, R. Hollatz, and U. Bergmann, Phys. Rev. Lett. **66**, 770 (1991).
[15]D. P. Siddons, U. Bergmann, and J. B. Hastings, Phys. Rev. Lett. **70**, 359 (1993).
[16]E. E. Alp, T. M. Mooney, T. Toellner, W. Sturhahn, E. Witthoff, R. Röhlsberger, E. Gerdau, H. Homma, and M.

Kentjana, Phys. Rev. Lett. **70**, 3351 (1993).
[17]J. P. Hannon and G. T. Trammell, Phys. Rev. **169**, 315 (1968).
[18]J. P. Hannon and G. T. Trammell, Phys. Rev. **186**, 306 (1969).
[19]A. M. Afanas'ev and Y. Kagan, Zh. Eksp. Teor. Fiz. **45**, 1660 (1963) [Sov. Phys. JETP **20**, 1139 (1964)].
[20]Y. Kagan and A. M. Afanas'ev, Zh. Eksp. Teor. Fiz. **47**, 1108 (1964) [Sov. Phys. JETP **20**, 743 (1965)].
[21]W. Sturhahn, Ph.D. dissertation, Hamburg, 1991.
[22]S. Margulies and J. R. Ehrmann, Nucl. Instrum. **12**, 131 (1961).
[23]S. M. Harris, Phys. Rev. **124**, 1178 (1961).
[24]The WOTAN program package is available from Dr. R. Hollatz, Klövensteenweg 54, 22559 Hamburg, Germany.
[25]The CONUSS program package is available form Dr. W. Sturhahn, Argonne National Laboratory, Advanced Photon Source, 9700 South Cass Av, Argonne, IL 60439, USA. E-mail: STURHAHN@oxygen.aps1.anl.gov.
[26]J. A. Ibers and W. C. Hamilton, *International Tables for X-Ray Crystallography* (Kluwer Academic, Dordreht, 1989), Vol. 4.
[27]D. L. Smith, *Empirical Formula for Interpolation of Tabulated Photon Photoelectric Cross Sections* (National Technical Information Service, Springfield, Virginia, 1971).
[28]M. E. Rose, *Elementary Theory of Angular Momentum* (Wiley, New York, 1957).
[29]H. C. Goldwire, Jr. and J. P. Hannon, Phys. Rev. B **16**, 1875 (1977).
[30]E. Matthias, W. Schneider, and R. M. Steffen, Ark. Fys. **24**, 97 (1963).
[31]P. J. Eberlein, Numer. Math. **14**, 232 (1970).
[32]U. Gonser and H. Fischer, *Resonance γ-Ray Polarimetry* (Springer-Verlag, Wien, 1981).
[33]R. Hollatz, Ph.D. dissertation, Hamburg, 1991.
[34]H. D. Rüter, R. Rüffer, E. Gerdau, R. Hollatz, A. I. Chumakov, M. V. Zelepukhin, G. V. Smirnov, and U. van Bürck, Hyperfine Interact. **58**, 2473 (1990).
[35]S. Kikuta, in *Proceedings of the International Conference on Anomalous X-Ray Scattering*, edited by K. Fischer, G. Materlik, and C. J. Sparks (Elsevier Science, New York, to be published).
[36]O. C. Kistner and A. W. Sunyar, Phys. Rev. Lett. **4**, 412 (1960).
[37]M. Seto (private communication).